Neuron, Vol. 15, 961–973, October, 1995, Copyright © 1995 by Cell Press

Glutamate-Induced Neuronal Death: A Succession of Necrosis or Apoptosis Depending on Mitochondrial Function

Maria Ankarcrona,* Jeannette M. Dypbukt,* Emanuela Bonfoco,* Boris Zhivotovsky,* Sten Orrenius,* Stuart A. Lipton,† and Pierluigi Nicotera*‡

*Institute of Environmental Medicine
Division of Toxicology
Karolinska Institute
Stockholm, Sweden 171 77
†Laboratory of Cellular and Molecular Neuroscience
Children's Hospital
and Program in Neuroscience
Harvard Medical School
Boston, Massachusetts 02115
‡Faculty of Biology
University of Konstanz
D-78465 Konstanz
Federal Republic of Germany

Summary

During ischemic brain injury, glutamate accumulation leads to overstimulation of postsynaptic glutamate receptors with intracellular Ca^{2+} overload and neuronal cell death. Here we show that glutamate can induce either early necrosis or delayed apoptosis in cultures of cerebellar granule cells. During and shortly after exposure to glutamate, a subpopulation of neurons died by necrosis. In these cells, mitochondrial membrane potential collapsed, nuclei swelled, and intracellular debris were scattered in the incubation medium. Neurons surviving the early necrotic phase recovered mitochondrial potential and energy levels. Later, they underwent apoptosis, as shown by the formation of apoptotic nuclei and by chromatin degradation into high and low molecular weight fragments. These results suggest that mitochondrial function is a critical factor that determines the mode of neuronal death in excitotoxicity.

Introduction

Intracellular Ca^{2+} overload, concomitant generation of free radicals, and depression of cell energy metabolism are thought to play important roles in the pathogenesis of ischemic brain damage (Choi, 1988, 1995; Meldrum and Garthwaite, 1990; Coyle and Puttfarcken, 1993; Lipton and Rosenberg, 1994). During focal cerebral infarction, neurons in the center of the ischemic region rapidly die. In contrast, more distant neurons in the penumbra, although prone to injury, remain viable for several hours (Siesjö, 1992). A similar type of delayed neuronal cell death is observed after exposure to excitatory amino acids in specific neuronal subpopulations, either in vitro or in vivo, including retinal ganglion cells, cerebellar granule cells, and hippocampal cortical neurons (Hahn et al., 1988; Manev et al., 1989; Choi and Rothman, 1990; Garthwaite and Garthwaite, 1990).

The morphological characteristics of excitotoxic injury in vivo (i.e., swelling of the cell soma and the dendrites) are consistent with a necrotic type of death. However, recent studies have provided evidence that some neuronal subpopulations may die via apoptosis following the activation of an endogenous cell death program (Kure et al., 1991; Héron et al., 1993; Linnik et al., 1993; MacManus et al., 1993, 1994). Necrosis and apoptosis are two distinct forms of cell death that have profoundly different implications for the surrounding tissue. Necrosis is a passive process, typified by cell and organelle swelling with spillage of the intracellular contents into the extracellular milieu. The result of this process is usually an inflammatory reaction that leads to local cellular infiltration, vascular damage, edema, injury to the surrounding tissue, and, eventually, fibrosis. In contrast, apoptosis is characterized by cell shrinkage, organelle relocalization and compaction, chromatin condensation, and production of membrane-enclosed particles containing intracellular material known as "apoptotic bodies" (Kerr et al., 1972; Wyllie et al., 1980; Arends and Wyllie, 1991). In vivo, phagocytic cells normally sequester antigenically modified apoptotic cells, preventing inflammation and damage to the surrounding tissue (Duvall et al., 1985; Savill et al., 1993).

While the distinction between the two types of cell death is obvious in certain systems, in others the coexistence of cells with either necrotic or apoptotic features makes it difficult to determine the predominant mechanism of death. Further complication comes from the observation that secondary necrosis may take place in apoptotic model systems either in vitro or in vivo when an unusually large number of cells undergo apoptosis at a given time (Leist et al., 1995). This may simply reflect an insufficient removal of apoptotic cells by phagocytes. In this case, secondary processes may cause cell disintegration, mimicking necrosis. Finally, the same type of insult can elicit either apoptosis or necrosis in several cell types, including neurons (Dypbukt et al., 1994; Bonfoco et al., 1995). For example, in cortical cultures $NO^{\cdot}$ reacting with $O_2^{\cdot -}$ to form peroxynitrite elicits neuronal apoptosis with mild insults but elicits necrosis with increasing intensity of exposure (Bonfoco et al., 1995). Thus, knowing the inciting stimulus or even the final pathological outcome does not always guarantee one's ability to decipher the proper mechanism of cell death.

In attempting to define the events resulting in these two forms of cell death, it is therefore mandatory to analyze all the distinguishing features of apoptosis and necrosis as they develop temporally within a single-cell system. This prompted us to study the type of cell death resulting from the exposure of a single neuronal population to glutamate. As a model, we used primary cultures of cerebellar granule cells. Such cultures contain virtually a single-cell population (Vaccarino et al., 1987) that possesses

N-methyl-D-aspartate (NMDA)–type channels (Schramm et al., 1990). In these cells, glutamate toxicity can be exclusively attributed to the overstimulation of the NMDA subtype of receptor, leading to Ca^{2+} overload (Schramm et al., 1990). Our results show that both forms of neuronal cell death occur after exposure to glutamate. First, a rapid necrotic cell killing occurs during and immediately after glutamate exposure and is associated with loss of mitochondrial function. Second, a delayed apoptotic type of neuronal death occurs in the surviving neurons that recover their mitochondrial function and cellular energy levels.

Results

Glutamate Induces Rapid Cell Death in a Neuronal Subpopulation

In all experiments, cerebellar granule cells were exposed to different glutamate concentrations (1 μM to 3 mM) for 30 min and subsequently reincubated in culture medium lacking glutamate. As judged by trypan blue uptake and by a decreased ability to metabolize MTT to formazan, glutamate caused dose-dependent neuronal cell killing with a rapid onset. Depending on the concentration, 25%–50% of the neurons died within the first 3 hr following exposure (Figures 1A and 1B). Conversely, no further inhibition of MTT metabolism (Figure 1A) or increase in trypan blue uptake (data not shown) occurred between 3 and 24 hr. Following a recovery period of 30 min, reexposure to glutamate induced a second wave of rapid killing of the surviving neurons (Figure 1B). The NMDA receptor/channel antagonist MK-801 protected cells from this glutamate-induced neuronal death (Figure 1C).

Early Neuronal Cell Killing Is Preceded by Loss of Mitochondrial Membrane Potential

Changes in mitochondrial membrane potential were monitored in individual neurons by determining the shift in fluorescence emission and the intensity of the dye JC-1 (see Experimental Procedures) (Reers et al., 1991).

The inner mitochondrial membrane possesses a negative potential on the matrix side. Thus, lipophilic molecules with a positive charge accumulate in the matrix as a function of membrane potential (Smiley et al., 1991). Accordingly, the fluorescent green dye JC-1 monomer accumulates in the mitochondrial matrix. When JC-1 exceeds a critical concentration, the dye molecules form J-aggregates. This is accompanied by a shift in the absorption and fluorescence maximum to longer wavelengths, resulting in a red emission peak (Reers et al., 1991). The formation of J-aggregates in mitochondria is dependent upon the presence of an intact electrochemical gradient (Smiley et al., 1991). Agents that abolish the normal electrochemical gradient, depolarize the membrane, and thereby deenergize mitochondria (e.g., protonophores or antimycin A) cause the loss of the red fluorescence. In contrast, the monomer green fluorescence is less sensitive to membrane potential changes; JC-1 monomer is not completely released from deenergized mitochondria (Reers et al., 1991). How-

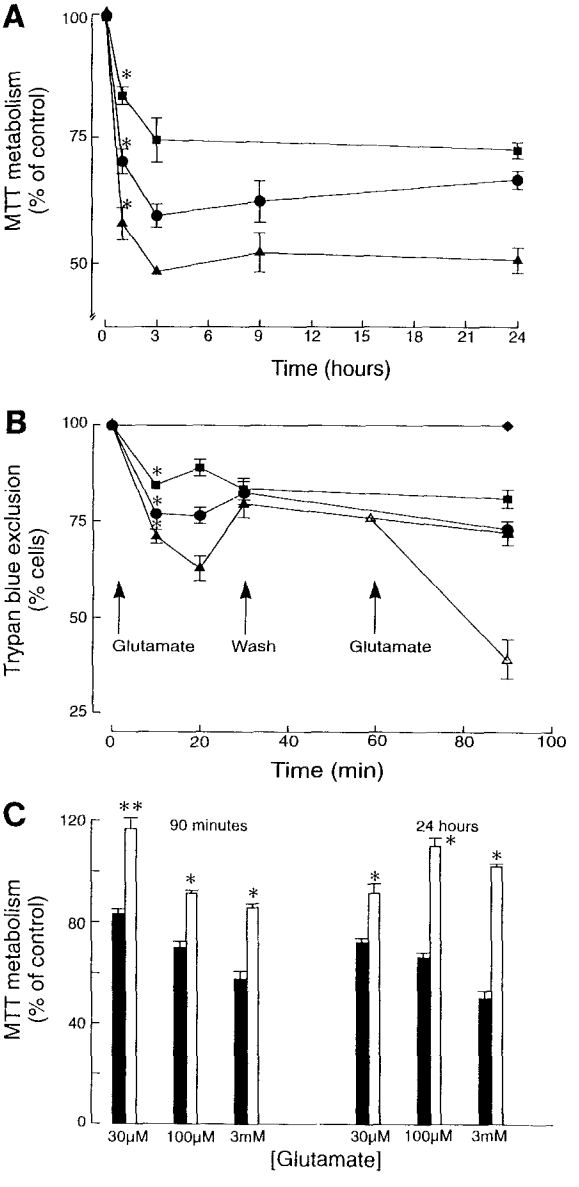

Figure 1. Glutamate Induces Death of Cerebellar Granule Cells

Neurons were exposed to different concentrations of glutamate for 30 min and then incubated in growth medium.

(A) MTT assay with 30 μM glutamate (squares), 100 μM glutamate (circles), and 3 mM glutamate (triangles). Results are expressed as a percentage of control cultures not exposed to glutamate.

(B) Rapid disruption of plasma membrane permeability assayed by trypan blue exclusion; glutamate concentrations were 1 μM (diamonds), 30 μM (sqares), 100 μM (circles), 3 mM (closed triangles), and 3 mM added a second time after a wash and a 30 min recovery period (open triangles). Note that the loss of viability indicated by the trypan blue assay is less pronounced than that displayed in the MTT assay in (A). This may reflect a decrease in mitochondrial function in the subpopulation of neurons that will not undergo necrosis and later recover their energy level (see Figure 2). The apparent recovery of viability with the trypan blue assay after 20 min reflects the disappearance of necrotic cells that rapidly fragmented, as shown in Figure 4.

(C) Glutamate toxicity (closed bars) is ameliorated by MK-801 (1 μM; open bars), measured by the MTT assay. All values are mean ± SD of three to six separate experiments. Asterisk indicates significantly different ($p < .05$) from control (A and B) or from samples without MK-801 (C).

ever, permeabilization of the membrane reduces JC-1 accumulation in the mitochondria and eventually results in the disappearance of both red and green fluorescence (Smiley et al., 1991).

In viable cells, including neurons, mitochondrial subpopulations with differing membrane potentials can be identified using the property that JC-1 produces green fluorescence at depolarized potentials (positive to −100 mV) and red-orange fluorescence at hyperpolarized potentials (more negative than −140 mV) (Chen and Smiley, 1993).

In neurons preloaded with JC-1, high and low energy mitochondrial subpopulations displayed a heterogeneous distribution, with red fluorescence primarily localized in the dendritic projections and green fluorescence around the cell somas, respectively. After exposure to 3 mM glutamate, the mitochondrial membrane potential rapidly depolarized (Figures 2a–2d), as shown by the disappearance of the red-stained mitochondria within a few minutes. The low energy subpopulation that originally stained green was initially retained. Locally, mainly around the cell bodies, the green fluorescence then increased. This was most likely the result of intra-mitochondrial accumulation of JC-1 monomers from dissolving J-aggregates. After 30 min, the green fluorescence was conserved around the cell somas and, to a lesser extent, in the projections of some neurons, but had disappeared in others. To find out whether cell permeabilization had occurred in the latter neurons during the exposure to glutamate, cultures were superfused with the red dye, propidium iodide. As shown in Figure 2e, in addition to neurons that retained the green fluorescence and excluded propidium, others stained red with propidium, indicating loss of membrane integrity after glutamate.

Quantitatively, exposure to 3 mM glutamate for 30 min resulted in propidium iodide uptake in 38% ± 4% of the cerebellar granule cells. As a control, when the surviving neurons were artificially permeabilized with the detergent Triton X-100, residual JC-1 staining was lost and additional propidium-stained nuclei appeared (Figure 2f). Collectively, these experiments indicate that within minutes of glutamate exposure a subpopulation of cerebellar granule cells lost mitochondrial membrane potential and viability. A second subpopulation of cerebellar granule cells (i.e., those impermeable to propidium iodide prior to Triton X-100 treatment) survived and retained a low energy mitochondrial population, as shown by the green JC-1 fluorescence.

To investigate whether further changes in mitochondrial membrane potential and neuronal viability would follow glutamate removal, we performed another set of experiments. Cerebellar granule cells loaded with JC-1 and exposed to glutamate for 30 min as above were washed and then reincubated in fresh medium (Figures 2g and 2h). Similar to the above results, only a minority of the neurons lost mitochondrial membrane potential and viability within the first hour. The majority of neurons fully recovered mitochondrial membrane potential, as shown by the reappearance of the J-aggregates (red fluorescence) in the neuronal projections (Figure 2h). If glutamate was then added again to the cultures, a second immediate depolarization in mitochondrial membrane potential was observed, indicated by the green fluorescence of JC-1 monomers (Figure 2i). This was followed by a second wave of neuronal cell death, evident in the loss cf green fluorescence due to membrane leakage (Figures 2j–2l) and the lack of trypan blue exclusion (see Figure 1B).

By measuring ATP, ADP, and AMP levels in the neuronal cultures, we also detected a marked decrease of cell energy charge during and shortly after glutamate exposure. Subsequently, however, between 3 and 12 hr after glutamate exposure, the population surviving the early phase of neuronal cell death recovered energy charge (Figure 3).

Neuronal Death during and Immediately after Exposure to Glutamate Occurs by Necrosis

The next set of experiments was performed to decide whether the initial neuronal cell killing was of the necrotic or apoptotic type. Cerebellar granule cells loaded with the membrane-permeant chromatin dye SYTO-13 were exposed to glutamate in the presence of the membrane-impermeant chromatin dye propidium iodide. While neurons with intact membranes retained the green (SYTO-13) fluorescence and excluded propidium iodide, nuclei of neurons with damaged membranes were progressively stained by propidium iodide and shifted to red as the dye intercalated with DNA (Figures 4a–4e). Concomitantly, red debris appeared as nucleic acids were scattered into the extracellular medium. Notably, the nuclear size of the permeabilized dying neurons swelled from 3.7 ± 0.4 to 4.6 ± 0.6 μm (mean ± SD; n = 30 cells scored; $p < .05$ by paired Student's t test). Following the removal of glutamate and reincubation in fresh medium, many large, propidium-stained nuclei were visible in the same field as apparently unaffected nuclei that retained the green SYTO-13 stain (Figure 4f). These results show that, during and shortly after glutamate exposure, a subpopulation of cerebellar granule cells died by necrosis.

Surviving Neurons Undergo Delayed Cell Death by Apoptosis

We next decided to investigate the fate of neurons that survived the early phase of glutamate exposure. Cerebellar granule cells were incubated in glutamate for 30 min, followed by normal medium for 6 hr. The neurons were then loaded with SYTO-13 and placed in normal medium in the presence of propidium iodide. Within 6 hr of glutamate exposure, several neurons developed condensed chromatin in pyknotic nuclei (Figure 4g). These neurons excluded propidium iodide; i.e., they had intact cell membranes and thus retained green fluorescence. Such neurons also exhibited an increased resistance to detergent-induced membrane lysis. This was illustrated by the fact that Triton X-100 at concentrations up to 1% (v/v) did not promote a fluorescence shift in the pyknotic cells in the presence of extracellular propidium iodide. A concentration as high as 10% Triton X-100 was required to increase nuclear penetration of propidium iodide, resulting in the yellow

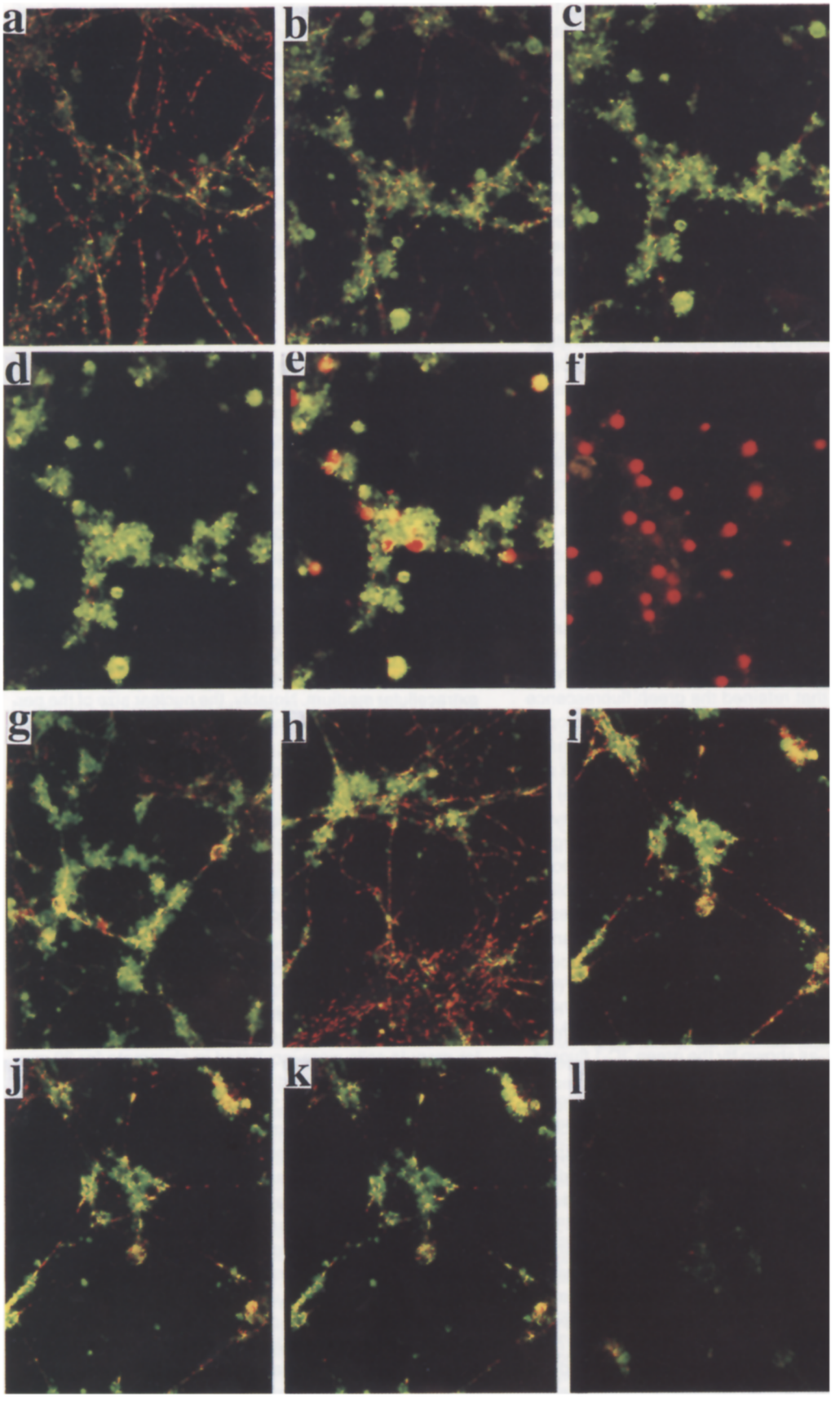
a
b
c
d
e
f
g
h
i
j
k
l

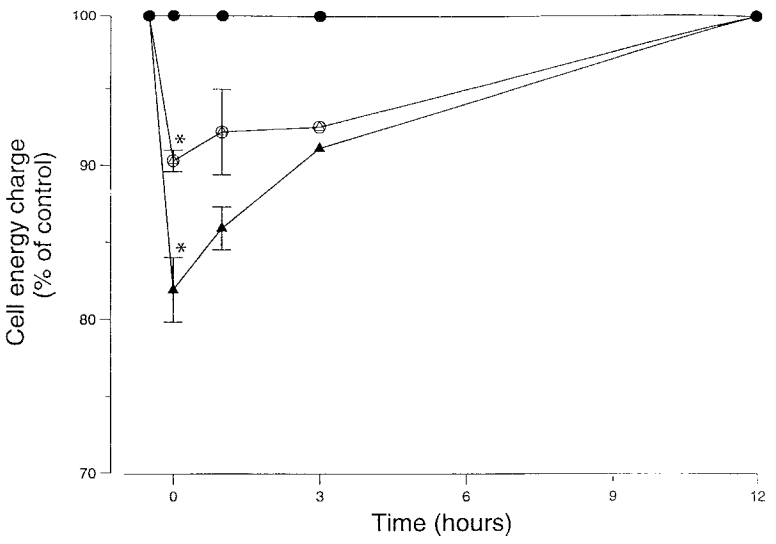

Figure 3. Glutamate Causes a Transient Loss of Neuronal Cell Energy Charge

Neurons were exposed to various concentrations of glutamate for 30 min and then incubated in culture medium for the times shown on the X axis (closed circles, control; open circles, 30 μM glutamate; open triangles, 100 μM glutamate; closed triangles, 3 mM glutamate). Intracellular levels of ATP, ADP, and AMP, as well as energy charge, were determined as described in Experimental Procedures. Results are expressed as the mean ± SD from three different experiments. Asterisk, significantly different ($p < .05$) from control.

fluorescence observed in Figure 4h. The yellow color was produced by the superimposition of the red (propidium iodide) and green (SYTO-13) dyes. In contrast, neurons exhibiting green fluorescence, retaining normal size, and initially excluding propidium iodide (i.e., the apparently normal neurons) were rapidly stained red upon the addition of Triton X-100 at concentrations as low as 0.5%–1% (data not shown). In these normal neurons, membrane permeabilization with low or high concentrations of Triton X-100 allowed the entry of such large amounts of propidium iodide that the red fluorescence dominated (Figure 4h).

As shown in Figure 5, in the hours following glutamate exposure, there was a progressive increase in the number of neurons displaying chromatin condensation and formation of typical apoptotic nuclei. After exposure to 3 mM glutamate, nearly all neurons had apoptotic nuclei within 6–12 hr (Figures 5d–5f and 6). Lower, micromolar concentrations of glutamate required 24 hr to produce similar apoptotic effects (Figures 5b, 5c, and 6). The number of apoptotic cells increased in a dose-dependent fashion (Figure 6). At the lowest concentration (1 μM), which did not induce necrosis (see Figure 1B), glutamate still promoted apoptosis in 10% of the population by 24 hr. Blockade of NMDA receptor–operated channels by MK-801 protected neurons from apoptosis, suggesting that Ca^{2+} influx through these channels was the initial trigger for the delayed apoptotic cell death (Figure 6).

In addition, unlike necrotic neurons, cerebellar granule cells undergoing apoptosis remained adherent to the culture dish and retained their processes. Thus, apoptotic nuclei could be seen in otherwise apparently normal neurons. In this preparation, after glutamate insult leading to apoptosis, the neurofilaments remain intact (Figure 7). However, we cannot preclude the involvement of other cytoskeletal proteins in the apoptotic process, e.g., the nuclear lamins (Ankarcrona et al., unpublished data).

High and Low Molecular Weight DNA Fragments in Neuronal Apoptosis

During apoptosis of various cell types, chromatin is degraded into high and low molecular weight fragments (Wyllie, 1980; Brown et al., 1993; Oberhammer et al., 1993; Zhivotovsky et al., 1994a, 1994b). In the present experiments, we show that glutamate-treated neurons surviving the initial necrotic phase of cell death undergo progressive DNA cleavage into 700, 300, and finally 50 kb fragments, as detected by field-inverted electrophoresis (Figure 8A). MK-801 prevented the cleavage of chromatin into these fragments (Figure 8B). During apoptosis, formation of the

Figure 2. Glutamate Induces Loss of Mitochondrial Membrane Potential in Cerebellar Granule Cells

Neurons were loaded with JC-1 as described in Experimental Procedures. The dye is not retained by cells that become permeabilized.

(a) Before the addition of glutamate, peripheral mitochondria fluoresced red, indicating a hyperpolarized membrane potential, while mitochondria in cell somas and some processes stained green, indicating more depolarized potentials.

(b–d) Neurons were exposed to 3 mM glutamate, and images were collected as described in Experimental Procedures at 10, 15, and 30 min.

(e) Glutamate was washed out, and neurons were superfused with medium containing propidium iodide (10 μg/ml). Cells with damaged membranes lost their JC-1 fluorescence and took up propidium iodide, yielding a red fluorescence.

(f) After addition of Triton X-100 (0.5%), all neurons were permeabilized and stained red by propidium iodide. The JC-1 staining disappeared upon permeabilization.

(g) Another group of neurons was exposed to glutamate for 30 min.

(h) Subsequent reincubation for 30 min resulted in restoration of the mitochondrial membrane potential, shown by the presence of many processes exhibiting red fluorescence.

(i–l) The second addition of 3 mM glutamate again caused a loss JC-1 fluorescence, illustrated immediately after exposure to glutamate and at 5, 10, and 15 min.

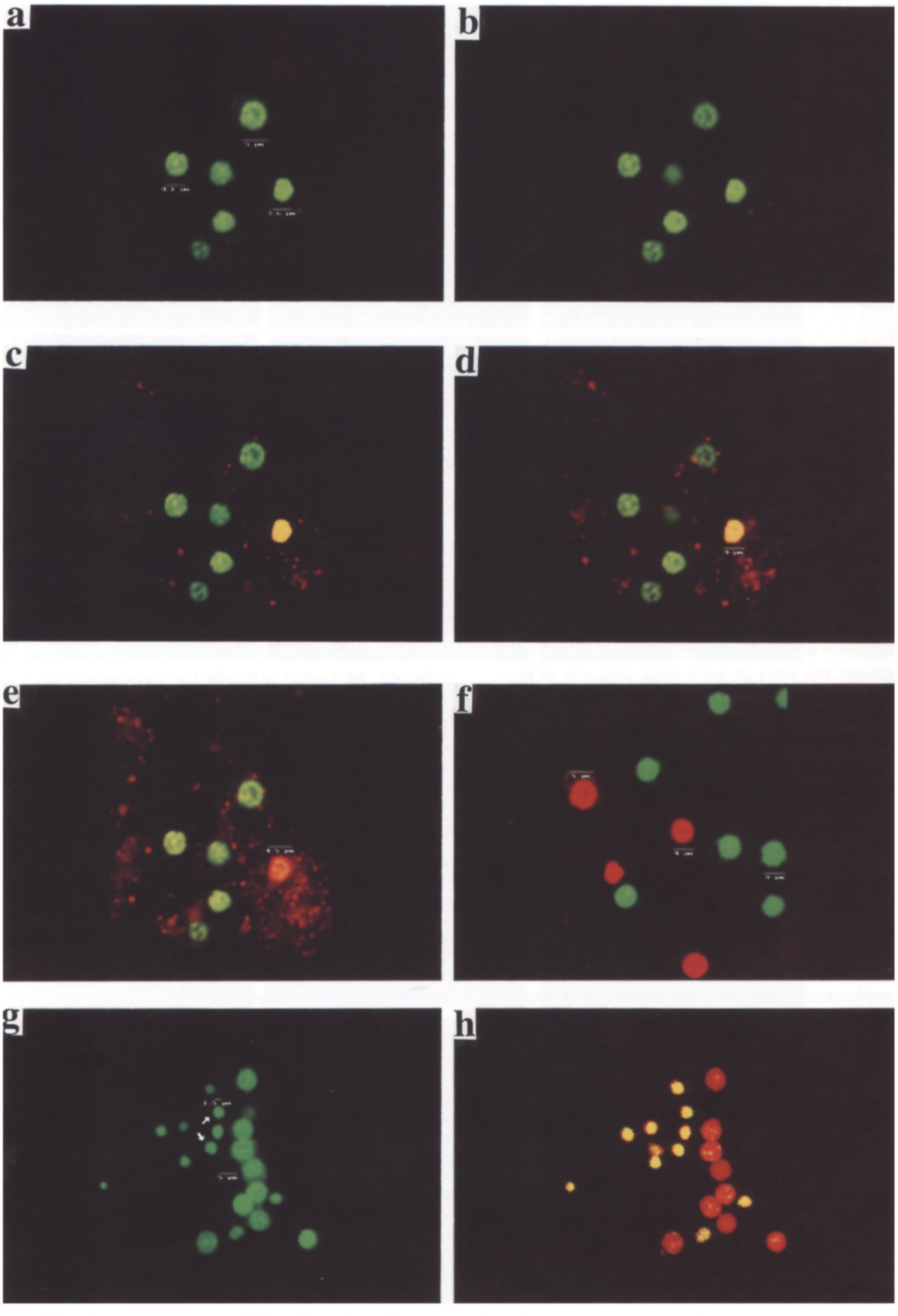
a
b
c
d
e
f
g
h

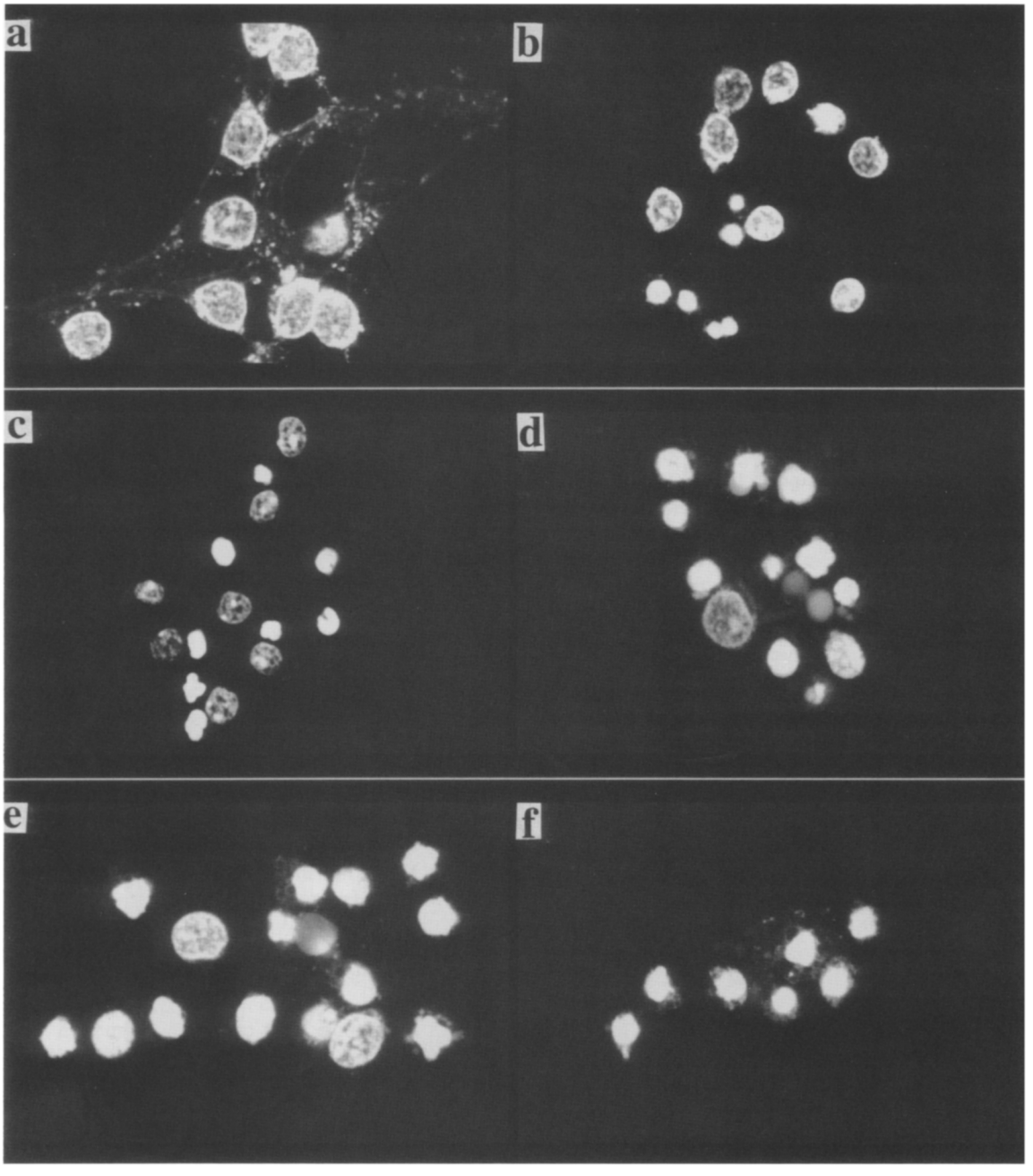

Figure 5. Cerebellar Granule Cells Exposed to Glutamate Undergo Chromatin Condensation

Neurons were exposed to various concentrations of glutamate for 30 min and then incubated in culture medium for the times indicated below. The cultures were then fixed, permeabilized, stained with propidium iodide, and examined by confocal microscopy. (a) Control at 24 hr; (b) 30 μM glutamate at 24 hr; (c) 100 μM glutamate at 24 hr; (d) 3 mM glutamate at 6 hr; (e) 3 mM glutamate at 9 hr; (f) 3 mM glutamate at 12 hr. Note that in (b) and (d) some preapoptotic nuclei exhibiting chromatin buttoning can be seen near typically condensed nuclei.

Figure 4. Necrosis and Apoptosis of Cerebellar Granule Cells Stimulated by Glutamate

(a–e) Neurons were loaded with 0.5 μM SYTO-13 and exposed to glutamate in the presence of propidium iodide (10 μg/ml). Neurons that died by necrosis progressively exhibited a fluorescence shift from green to orange-red because propidium iodide gained entry into the nucleus. Nuclei did not become pyknotic. Instead, they swelled and then fragmented, spreading genetic material (stained in red by propidium iodide) into the surrounding medium (a, control; b–d, after a 7 min [b], 10 min [c], 15 min [d], or 30 min [e] exposure to 3 mM glutamate). In the field illustrated in (a)–(e), a single neuron developed propidium iodide staining. The diameter of the nucleus increased from 3.6 μm under control conditions to 4.5 μm. Simultaneously, red debris appeared from the neurons just outside of the field that had also undergone necrosis.

(f) Another field after a 30 min exposure to glutamate followed by a wash to remove debris. The number of neurons stained by propidium iodide in this manner was counted in ten fields in three separate experiments (more than 400 neurons scored). After a 30 min exposure to 3 mM glutamate, a significant number of neurons underwent necrosis (38% ± 4%, mean ± SD; $p < .05$ by Student's t test).

(g and h) Cerebellar granule cells surviving early glutamate exposure undergo delayed nuclear condensation typical of apoptosis. Neurons loaded with SYTO-13 were imaged 6 hr after exposure to glutamate. Propidium iodide (10 μg/ml) was included in the incubation medium. Apparently normal neurons had larger nuclear diameters than apoptotic nuclei, which also lacked discernible chromatin structure (g). Normal nuclei in this experiment had diameters of 3.8 ± 0.6 μm (mean ± SD; $n = 30$). Apoptotic nuclei were significantly smaller, averaging 1.7 ± 0.2 μm ($n = 30$; $p < .05$ by Student's t test). As shown in (h), permeabilization with high concentrations of Triton X-100 (10%) produced partial staining of apoptotic nuclei with propidium iodide (shift toward yellow-orange fluorescence) and complete staining of apparently normal nuclei (red fluorescence).

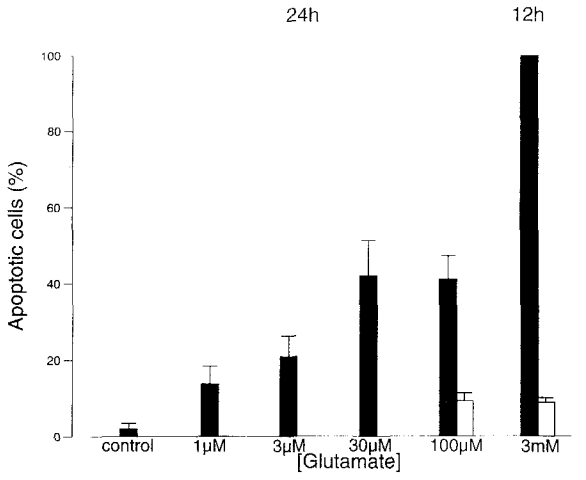

Figure 6. Formation of Apoptotic Nuclei in Cerebellar Granule Cell Cultures after Exposure to Glutamate: Time and Dose Dependence

Neurons were fixed, permeabilized, stained with propidium iodide, and examined by confocal microscopy. Glutamate exposure (closed bars) versus glutamate exposure in the presence of 1 μM MK-801 (open bars). Results are expressed as mean ± SD (n = 4). Asterisk indicates statistically different ($p < .05$) from control or from sample without MK-801. Ten fields or more than 400 cells were scored for each sample.

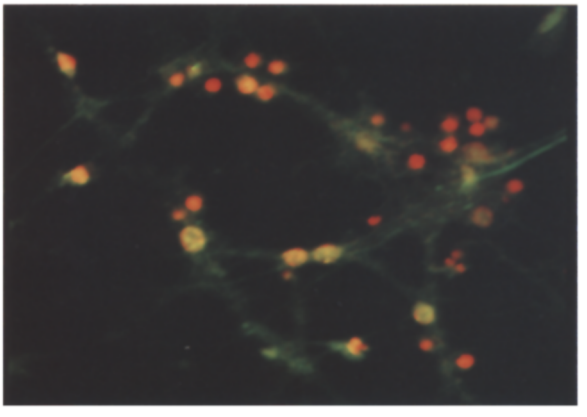

Figure 7. Staining of Neurofilaments and Nuclei in Cerebellar Granule Cells Exposed to Glutamate Reveals Intact Neurites in Apoptotic Neurons

Cultures were exposed to 100 μM glutamate for 30 min and subsequently reincubated in their original culture medium for 24 hr. The neurons were then fixed in methanol and incubated with a monoclonal antibody to the neurofilament-200 subunit (Sigma). This was followed by incubation in secondary antibody conjugated to fluorescein (goat anti-mouse IgG, FITC-coupled, affinity-purified F(ab')2 fragments; Jackson ImmunoResearch Laboratories). The nuclei were then stained with 20 μM ethidium homodimer (Molecular Probes). Images were visualized with a Bio-Rad confocal microscope using the 488 nm excitation line and the K1 and K2 filter blocks. Neurofilaments fluoresce green and nuclei fluoresce red. Note that the apoptotic neurons, containing the shrunken red nuclei, still have intact green neurites, as labeled with anti-neurofilament antibody. In addition, the apoptotic nuclei are attached to the neurofilaments.

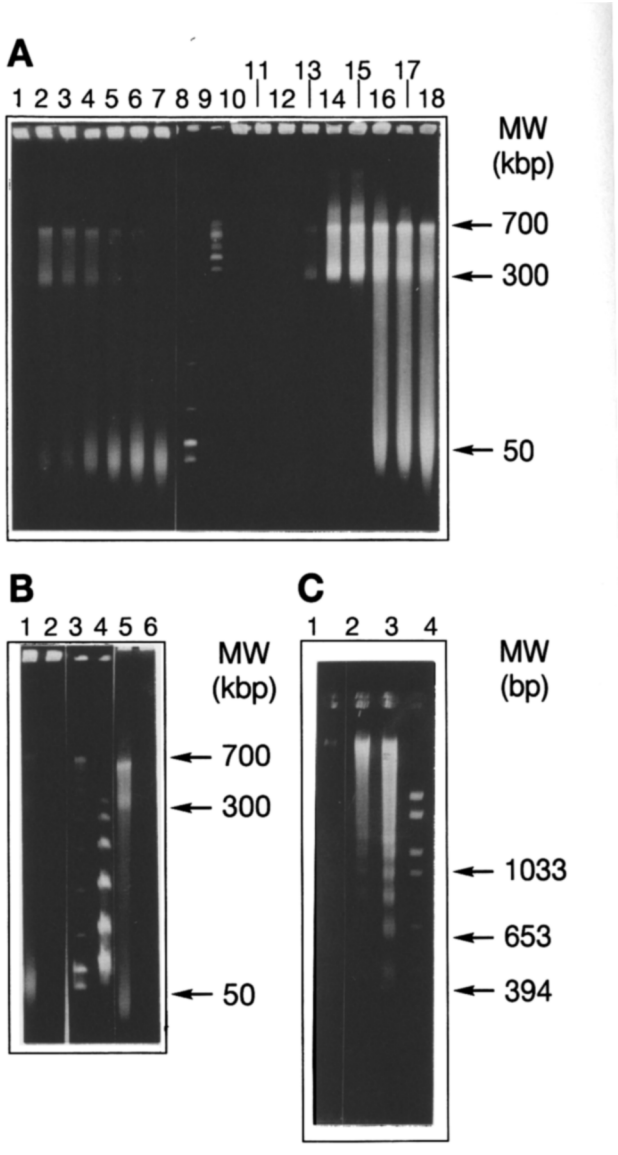

Figure 8. Progressive Formation of Large and Small DNA Fragments in Cerebellar Granule Cells Exposed to Glutamate for 30 min

(A) Time course of the appearance of large-size DNA fragments as detected with field-inverted gel electrophoresis. Lane 1: control after 48 hr; lanes 2–7: 6, 9, 12, 18, 24, and 48 hr, respectively, after exposure to 100 μM glutamate; lanes 8 and 9: DNA markers; lanes 10–18: 0.5, 1, 3, 6, 9, 12, 18, and 24 hr, respectively, after exposure to 3 mM glutamate.

(B) Protection from the formation of high molecular weight DNA fragments by MK-801 (1 μM). Lane 1: 24 hr after exposure to 100 μM glutamate; lane 2: 24 hr after exposure to 100 μM glutamate plus MK-801; lanes 3 and 4: DNA markers; lane 5: 12 hr after exposure to 3 mM glutamate; lane 6: 12 hr after exposure to 3 mM glutamate plus MK-801

(C) Conventional agarose gel electrophoresis was used to detect the formation of oligonucleosomal DNA fragments (DNA laddering). Lane 1: control at 24 hr; lane 2: 24 hr after exposure to 1 mM glutamate; lane 3: 24 hr after exposure to 3 mM glutamate; lane 4: DNA markers.

50 kb fragments occurred concomitantly with chromatin condensation. In contrast to these findings, field-inverted electrophoresis did not reveal high molecular weight DNA fragmentation during the rapid initial phase of necrotic cell killing by glutamate (Figure 8A).

Subsequent to the formation of high molecular weight DNA fragments in neurons undergoing apoptosis, oligonucleosomal-sized (<2000 bp) fragments were detected by conventional agarose gel electrophoresis. This oc-

curred in neurons initially surviving exposure to the highest (1 or 3 mM) glutamate concentrations (Figure 8C). DNA laddering was detected on these conventional agarose gels only at later times (e.g., 24 hr after glutamate exposure).

Neurons exposed to lower glutamate concentrations also underwent apoptosis (Figures 5, 8A, and 8B). They did not, however, exhibit conventional DNA laddering even at later time points (i.e., 24 or 48 hr). These findings are consistent with the notion that, although oligonucleosomal DNA fragmentation remains a typical marker for apoptosis when it is present, it is not a prerequisite for the formation of apoptotic nuclei (Cohen et al., 1992; Brown et al., 1993; Oberhammer et al., 1993). Here we have extended this concept to neurons.

Discussion

In this study we have shown that cerebellar granule cells exposed to neurotoxic concentrations of glutamate undergo two distinct fates: a subpopulation succumbs to acute necrosis during and immediately after the exposure, while the remaining neurons die from delayed-onset apoptosis. The intensity of the glutamate exposure and the resulting effects on mitochondrial function are critical factors in determining which of the two pathways to neuronal cell death is followed. The findings regarding the intensity of the insult are consistent with previous hypotheses (Choi, 1995) and our recent observations on cortical neurons (Bonfoco et al., 1995). More importantly, our data demonstrate that relatively intact mitochondrial activity of neurons appears to be necessary for the apoptosis program to proceed. Under our conditions, a very mild insult (e.g., a 30 min exposure to 1 μM glutamate) resulted in an insignificant degree of immediate necrosis and only a small incidence of delayed apoptosis. With higher concentrations of glutamate, an increasing proportion of neurons rapidly lost mitochondrial membrane potential and energy charge, and then died by necrosis. The surviving population, which recovered energy levels and mitochondrial membrane potential, subsequently succumbed to delayed-onset apoptosis. In our experiments, apoptotic nuclei were observed in neurons that had an active mitochondrial metabolism, as judged, for example, by the conserved ability to convert MTT to formazan even after 24 hr.

Despite recent advances in research on the molecular determinants of cell death, the distinction between necrosis and apoptosis still relies primarily on morphological criteria. In the present study, differences between the early necrotic phase and the delayed apoptotic component were obvious. Neuronal necrosis was characterized by swelling of the nucleus and spillage of genomic material into the extracellular medium. Prior to these events, dying neurons rapidly lost their mitochondrial membrane potential, energy charge, and, subsequently, the ability to metabolize MTT or to exclude trypan blue. The absence of chromatin condensation, pyknotic nuclei, and high molecular weight DNA fragments indicates that apoptosis did not occur (Brown et al., 1993; Nicotera et al., 1994; Zhivotovsky et al., 1994a).

In contrast, in neurons surviving the initial necrotic insult, the following typical features of apoptosis developed with a slow time course. First, within 3–6 hr of 100 μM to 3 mM glutamate exposure, we observed the accumulation of large 700 and 300 kb DNA fragments on agarose gels and visualized chromatin buttoning by confocal microscopy (see Figure 5); these events represent a prelude to chromatin condensation (Cohen et al., 1993; Nicotera et al, 1994). Second, within 9–12 hr, 50 kb fragments had formed; this event appeared concomitantly with typically condensed, apoptotic nuclei. Third, within 24 hr, the appearance of small oligonucleosomal DNA fragmentation (known as DNA laddering) was observed, but only in neurons exposed to high (1–3 mM) concentrations of glutamate. Neurons exposed to lower (30–100 μM) glutamate concentrations did not display this pattern of oligonucleosomal DNA fragmentation, yet they still manifest apoptotic nuclei at 24 hr. Thus, similar to nonneuronal cells (Brown et al., 1993; Oberhammer et al., 1993), DNA laddering was not found to be a prerequisite for the formation of apoptotic nuclei in neurons. It is likely that the formation of large versus small (oligonucleosomal) DNA fragments involves distinct mechanisms (Zhivotovsky et al., 1994b), and lower glutamate concentrations simply did not trigger oligonucleosomal fragmentation.

In the case of high glutamate exposures, the formation of large followed by small DNA fragments may reflect the progressive cleavage of the chromatin superstructure: 300 kb fragments corresponding to rosette-like formations that contain six individual α-helical loops and 50 kb fragments corresponding to individual loop domains (Filipski et al., 1990). The mechanism involved in the formation of such fragments is still unclear; however, we have recently shown that activation of nuclear proteases and endonucleases is sufficient to reproduce this entire DNA fragmentation pattern observed in apoptosis (Zhivotovsky et al., 1994b).

Unlike excitotoxin-induced necrosis, neurons undergoing apoptosis due to glutamate remained adherent to the dish, with their projections intact. This finding is similar to that reported in neuronal apoptosis caused by withdrawal of trophic factors (Deckwerth and Johnson, 1994).

Another typical feature of apoptosis in nonneuronal cells is the sequestration of intracellular contents in membrane-enclosed bodies to prevent leakage into the surrounding tissue (Duvall et al., 1985). Similarly, in neurons we found that cerebellar granule cells undergoing apoptosis displayed an increased resistance to permeabilization with detergents. This could suggest a modification in the neurons' plasma membrane lipid composition or in protein–protein cross-linking, as observed in other apoptotic models in which Ca^{2+}-dependent transglutaminase is activated (Piacentini et al., 1991). However, we cannot exclude the possibility that the decreased accessibility of propidium iodide to the apoptotic nuclei was the result of changes in the nuclear envelope or in chromatin accessibility.

Chromatin alterations appeared relatively early in our experimental model of apoptosis. While nuclear changes in apoptosis may be secondary to the activity of cytoplasmic (Jacobson et al., 1994; Lazebnik et al., 1994) or

mitochondrial (Newmeyer et al., 1994) factors, they arguably remain the most typical feature of the apoptotic process in nucleated cells. The cytoplasmic and nuclear changes observed during apoptosis imply an organized rearrangement of the cell structure involving cytoskeletal modifications (Oberhammer et al., 1994), volume changes (Thomas and Bell, 1981), and genome fragmentation (Wyllie et al., 1980; Zhivotovsky et al., 1994a). While not all these processes may directly require energy, a lack thereof would likely result in cell swelling and necrosis. ATP depletion, such as that caused by the combination of mitochondrial poisons and inhibitors of glycolysis, leads to loss of ion homeostasis, rapid blebbing, cell swelling, and lysis typical of necrosis (Nicotera et al., 1989). Following transient ischemia, ATP levels rapidly decline in certain neuronal populations, which swell and die (Arai et al., 1986). Conversely, in other neuronal populations, the initial ATP depletion is followed by a recovery to initial levels within 2 hr (Arai et al., 1986) and delayed neuronal death (Manev et al., 1989; Choi and Rothman, 1990; Garthwaite and Garthwaite, 1990). Delayed degeneration of cultured neurons after exposure to glutamate in vitro has been postulated to be similar in some respects to delayed neuronal death in vivo. During exposure to glutamate in our experiments, both mitochondrial membrane potential and ATP levels declined in many neurons. In those with irreversibly dissipated mitochondrial potentials, necrosis rapidly ensued. The surviving population recovered both mitochondrial membrane potential and energy levels and subsequently underwent delayed apoptosis. In this model system, such heterogeneous sensitivity to glutamate cannot be attributed to the coexistence of different neuronal subtypes. Heterogeneity within the same neuronal cell type, however, may result from different stages of development or different levels of expression of neuroprotective proteins. Following a 30 min exposure to glutamate, more resistant neurons may be rescued by removal of excitotoxin and/or readdition of fresh medium. Most importantly in our experiments, by the time DNA fragmentation and apoptotic nuclei were evident in neurons following glutamate exposure, mitochondrial membrane potential, metabolism, and energy charge had been restored to near normal levels. At this point, repeated challenge with glutamate resulted in repeated collapse of mitochondrial membrane potential, followed by necrosis. According to one hypothesis, loss of energy and onset of rapid necrosis simply prevents the activation of the "default" apoptotic program. This postulate is supported by the observation that treatment of cerebellar granule cells with the combination of 100 μM glutamate and the irreversible mitochondrial uncoupler carbonyl cyanide m-chlorophenylhydrazone (CCCP; 10 μM) resulted in necrosis of 60% of the neuronal population rather than in the delayed apoptosis observed with glutamate alone (Ankarcrona et al., unpublished data).

Heretofore, the role of mitochondria in apoptosis has remained unclear. The observation that apoptosis occurs in respiration-deficient cells had cast doubts on the role of mitochondrial energy production in apoptotic cell death (Jacobson et al., 1993). However, in that study glycolytic ATP production was sustained by supplementing the cultures with pyruvate. In another study, where mitochondrial factors had been suggested to induce the nuclear changes typical of apoptosis, inhibitors of mitochondrial respiration had little effect in preventing nuclear damage (Newmeyer et al., 1994). However, in that study an ATP regenerating system was included in the incubation medium, obfuscating the conclusions. Thus, prior to the present study, we still did not know whether neurons could die by apoptosis in the face of low energy levels.

Energy levels can easily be maintained by substrate supplementation in experimental model systems in vitro. Nevertheless, it is very difficult to envisage sufficient ATP generation under anaerobic conditions to maintain active cellular processes in neurons in vivo. Since mitochondria are the main source of ATP in mammalian cells, it is likely in the absence of substrate supplementation that collapse of mitochondrial membrane potential and impaired respiration would cause ATP depletion. Our experiments suggest that under these conditions necrosis intervenes before the apoptotic program has a chance to develop. It is tempting to speculate that mitochondrial energy generation is needed to maintain the osmotic integrity of the neuron via ion exchange mechanisms to avoid cell lysis. Nevertheless, a transitory Ca^{2+} overload of mitochondria could contribute to the generation of free radicals, which in turn may participate in the chain of events leading to delayed apoptosis (Bonfoco et al., 1995).

To date, most investigations concerning the possible involvement of apoptosis in excitotoxicity have used only one or two criteria to implicate this type of neuronal cell death. For example, based on sensitivity to cycloheximide or on detection of DNA laddering, several reports have either supported or excluded a role for apoptosis in ischemic neuronal injury (Kure et al., 1991; Ignatowicz et al., 1991; Dessi et al., 1993; Héron et al., 1993; Linnik et al., 1993; MacManus et al., 1993, 1994; Csernansky et al., 1994). However, the requirement for de novo protein synthesis, postulated in early studies on apoptosis, applies only to certain model systems (Wyllie et al., 1984; McConkey et al., 1989; Deckwerth and Johnson, 1993; Ratan et al., 1994) and not to others (Collins et al., 1991; Bellomo et al., 1992; Leist et al., 1994; Chow et al., 1995). The lack of DNA laddering is not per se diagnostic of the absence of apoptosis, as shown in the present study (see Figures 5 and 8). In view of these considerations, it is clearly not possible to distinguish apoptosis from necrosis using only one or two endpoints, and multiple criteria are necessary, as employed in the present study.

In conclusion, the type of cell death encountered in neuronal cultures exposed to glutamate may depend on the intensity of the exposure and may involve two temporally distinct phases. We believe that similar events could possibly occur in vivo after ischemic or other injuries. Necrosis, associated with extreme energy failure in mitochondria, may simply reflect the failure of neurons to carry out the "default" apoptotic death program used to dispose efficiently of aged or otherwise unwanted cells. The mainte-

nance of mitochondrial function may therefore be a decisive factor in determining the degree and progression of neuronal injury caused by excitotoxins.

Experimental Procedures

Chemicals

N-lauroylsarcosine, poly-L-lysine (MW 300,000), and 3-(4,5-dimethylthiazol-2-yl)-2,5-diphenyltetrazoliumbromide (MTT) were obtained from Sigma. Proteinase K was from Boehringer Mannheim. Agarose was obtained from FMC BioProducts. Dizocilpine (MK-801) was from Research Biochemicals, Inc. (Natick, MA). Propidium iodide, 5,5',6,6'-tetrachloro-1,1',3,3'-tetraethylbenzimidazolcarbocyanide iodide (JC-1), and SYTO-13 were purchased from Molecular Probes.

Neuronal Cell Cultures

Cerebellar granule cells were prepared from 7-day-old Sprague–Dawley rats as described by Schousboe et al. (1989). Neurons were seeded on poly-L-lysine (50 μg/ml)–coated dishes at a density of 0.25×10^6 cells/cm^2 and cultured in Eagle's Basal Medium (BME, GIBCO No. 21017) supplemented with 10% inactivated fetal calf serum, 25 mM KCl, 0.5% (v/v) penicillin–streptomycin. To prevent growth of glial cells, cytosine arabinoside (10 μM) was added to the cultures 48 hr after seeding. The sensitivity of cerebellar granule cells to glutamate increases with the number of days in culture (Frandsen and Schousboe, 1990). To ensure sensitivity to glutamate, we used 8- to 9-day-old cultures composed of >95% neurons (Vaccarino et al., 1987; Schramm et al., 1990). Cultures were exposed to glutamate for 30 min in a Locke solution (134 mM NaCl, 25 mM KCl, 4 mM $NaHCO_3$, 5 mM HEPES, 2.3 mM $CaCl_2$, 5 mM glucose) in the presence of 10 μM glycine. Since addition of fresh serum is toxic to cerebellar granule cells (Schramm et al., 1990), the neurons were reincubated in the old culture medium after exposure to glutamate. Neuronal cell death, measured as trypan blue uptake or formation of apoptotic nuclei, was negligible in control cultures. In experiments with MK-801, the antagonist was present 30 min before, during, and after exposure to glutamate.

Assessment of Necrosis and Apoptosis

Plasma membrane damage was assayed by the ability of cerebellar granule cells to take up trypan blue. In addition, we used the MTT tetrazolium salt assay to assess the integrity of mitochondrial enzymes in viable neurons. Normally, mitochondrial enzymes have the capacity to transform MTT tetrazolium salt into MTT formazan (Mosmann, 1983). In brief, MTT tetrazolium salt was dissolved in serum-free culture medium at a concentration of 0.3 mg/ml and then added to the neurons for 1 hr at 37°C. The medium was then aspirated, isopropanol was added, and aliquots were transferred to a 96-well plate. The absorbance was measured at 592 nm in a Labsystems Multiscan RMCC/340 plate reader. Results were expressed as the percentage of intact neurons compared with control. The MTT assay also provided an indication of mitochondrial metabolic function. A decrease in MTT metabolism correlated well with the loss of mitochondrial membrane potential and the decrease in energy level observed during the early necrotic phase after glutamate insult.

The mode of cell death, apoptosis versus necrosis, was determined in part using the combination of two fluorescent dyes, SYTO-13 and propidium iodide (Molecular Probes). Both dyes stain DNA; however, SYTO-13 is membrane permeant and yields green fluorescent chromatin, whereas propidium iodide is membrane impermeant and stains DNA red. Viable neurons displayed a normal nuclear size and green fluorescence. Necrotic neurons (i.e., cells succumbing to membrane lysis and spillage of their intracellular contents into the surrounding medium) manifest larger nuclei with red fluorescence. Apoptotic neurons (i.e., cells displaying pyknotic nuclei with condensed chromatin) had decreased nuclear diameters with green fluorescence and increased resistance to permeabilization with Triton X-100.

Fluorescence images were excited using the 488 nm line of a krypton/argon laser on a Bio-Rad MRC 600 fluorescent confocal microscope. Propidium iodide fluorescence was collected at its emission maximum of 617 nm (red), while SYTO-13 was collected at its emission maximum of 509 nm (green). Nuclear diameters were quantified using the Bio-Rad software, Comos.

In additional experiments, formation of apoptotic nuclei was assessed with propidium iodide after cells were permeabilized with methanol. Neurons grown on poly-L-lysine-coated coverslips were fixed in methanol:water (4:1) for 15 min, washed in phosphate-buffered saline, and subsequently stained with propidium iodide (5 μg/ml) for 5 min in the dark. The coverslips were mounted on glass slides in glycerol:HEPES-buffered saline (1:1) and examined under confocal microscopy. Nuclei of untreated cells revealed a typical chromatin morphology with distinct organization, whereas apoptotic nuclei appeared condensed and highly red fluorescent and displayed polarized chromatin aggregates.

Measurements of Mitochondrial Membrane Potential

In living cells, JC-1 exists either as a green fluorescent monomer at depolarized membrane potentials (positive to −100 mV) or as an orange-red fluorescent J-aggregate at hyperpolarized membrane potentials (negative to −140 mV) (Reers et al., 1991). JC-1 undergoes a reversible shift in emission, from 527 to 590 nm, as more J-aggregates form with increasingly negative mitochondrial membrane potential. Neurons cultured on glass coverslips were loaded with JC-1 (1.0 μg/ml) for 20 min at 37°C in culture medium containing 2% fetal bovine serum. Confocal, dual emission images were acquired at ten 1 s intervals for each time point to minimize photobleaching; at every fifth acquisition, two additional black and white images were obtained, stored in memory, and subsequently averaged to provide phase images of the field. In control experiments using these protocols, no photobleaching was observed when fluorescence was monitored at 0, 5, 10, 15, and 30 min.

Neuronal Cell Energy Charge

Intracellular ATP, ADP, and AMP concentrations were determined in neuronal cell extracts by high pressure liquid chromatography as described previously (Jones, 1981). Results were expressed as nanomoles per milligram of protein. Cell energy charge was calculated according to the following formula: (ATP + 0.5 × ADP)/(ATP + ADP + AMP) (Zubay, 1988). Mean control values for ATP, ADP, and AMP in untreated neurons were 1.44, 0.36, and 0.44 nmol/mg protein, respectively.

DNA Fragmentation into High and Low Molecular Weight Fragments

To monitor the formation of large-size DNA fragments (i.e., 50 kb), we performed field-inversion gel electrophoresis as previously described (Zhivotovsky et al., 1994b), using a horizontal gel chamber (HE 100B), power supply (PS 500 XT), and switchback pulse controller (PC 500, Hoefer Scientific), equipped with a constant temperature cooling system (Multitemp 2209, LKB). Electrophoresis was run at 180 V in 1% agarose gels at 12°C in 0.5 × TBE buffer (45 mM Tris, 1.25 mM EDTA, 45 mM boric acid [pH 8.0]), with the ramp rate changing from 20 to 30 s for the first 6 hr, 10 to 20 s for the second 6 hr, and 0.8 to 10 s for the next 12 hr, using a forward to reverse ratio of 3:1. Calibration of DNA sizes was performed using three sets of pulse markers with overlapping size ranges: chromosomes from Saccharomyces cerevisiae (225–2200 kb); 21 successive concatemers of DNA (50–1000 kb); and a mixture of DNA HindIII fragments, DNA, and DNA concatemers (0.1–200 kb). DNA was stained with ethidium bromide, visualized using a UV light source (305 nm), and photographed with Polaroid 665 positive negative film.

DNA fragmentation in oligonucleosomal fragments (DNA laddering) was detected by collecting the DNA released from the agarose plugs during incubation with proteinase K. This fraction was precipitated with 2 vol of absolute ethanol in the presence of 5 M NaCl. The DNA was subsequently loaded on conventional 1.8% agarose gels. Electrophoresis was run with constant current set at 60 mA. Gel staining and photography were performed as described above. DNA-size calibration was performed using DNA molecular weight marker VI (Boehringer-Mannheim). This marker is a mixture of fragments from pBR 328 DNA cleaved separately with BglI and HinfI. Fragment size was 154–2176 bp.

Acknowledgments

This work was supported in part by grants from the International Life Science Institute, the Swedish Natural Science Research Council (B-AA/BU 101 73-301), the Swedish Medical Research Council (03

X-2471), and the National Institutes of Health (P01 HD29587 and R01 EY09024).

The costs of publication of this article were defrayed in part by the payment of page charges. This article must therefore be hereby marked *"advertisement"* in accordance with 18 USC Section 1734 solely to indicate this fact.

Received February 16, 1995; revised May 23, 1995.

References

Arai, H., Passonneau, J. V., and Lust, W. D. (1986). Energy metabolism in delayed neuronal cell death of CA1 neurons of the hippocampus following transient ischemia in the gerbil. Metab. Brain Dis. *1*, 263–278.

Arends, M. J., and Wyllie, A. H. (1991). Apoptosis: mechanisms and roles in pathology. Int. Rev. Exp. Pathol. *32*, 223–254.

Bellomo, G., Perotti, M., Taddei, F., Mirabelli, F., Finardi, G., Nicotera, P., and Orrenius, S. (1992). Tumor necrosis factor α induces apoptosis in mammary adenocarcinoma cells by an increase in intranuclear free Ca^{2+} concentration and DNA fragmentation. Cancer Res. *52*, 1342–1346.

Bonfoco, E., Krainc, D., Ankarcrona, M., Nicotera, P., and Lipton, S. A. (1995). Apoptosis and necrosis: two distinct events induced respectively by mild and intense insults with *N*-methyl-D-aspartate or nitric oxide/superoxide in cortical cell cultures. Proc. Natl. Acad. Sci. USA *92*, 7162–7166.

Brown, D. G., Sun, X.-M., and Cohen, G. M. (1993). Dexamethasone-induced apoptosis involves cleavage of DNA to large fragments prior to internucleosomal fragmentation. J. Biol. Chem. *268*, 3037–3039.

Chen, L. B., and Smiley, S. T. (1993). Probing mitochondrial membrane potential in living cells by J-aggregate forming dyes. In Fluorescent and Luminescent Probes for Biological Activity: A Practical Guide to Technology for Quantitative Real-Time Analysis, W. T. Mason, ed. (New York: Academic Press), pp. 124–132.

Choi, D. W. (1988). Glutamate neurotoxicity and diseases of the nervous system. Neuron *1*, 623–634.

Choi, D. W. (1995). Calcium: still center-stage in hypoxic-ischemic neuronal cell death. Trends Neurosci. *18*, 58–60.

Choi, D. W., and Rothman, S. M. (1990). The role of glutamate neurotoxicity in hypoxic-ischemic neuronal death. Annu. Rev. Neurosci. *13*, 171–182.

Chow, S. C., Peters, I., and Orrenius S. (1995). Reevaluation of the role of *de novo* protein synthesis in rat thymocyte apoptosis. Exp. Cell Res. *216*, 149–159.

Cohen, G. M., Sun, X.-M., Snowden, R. T., Dinsdale, D., and Skilleter, D. N. (1992). Key morphological features of apoptosis may occur in the absence of internucleosomal DNA fragmentation. Biochem. J. *286*, 331–334.

Cohen, G. M., Sun, X.-M., Snowden, R. T., Ormerod, M. G., and Dinsdale, D. (1993). Identification of a transitional preapoptotic population of thymocytes. J. Immunol. *151*, 566–574.

Collins, R. J., Harmon, B. V., Souvlis, T., Pope, J. H., and Kerr, J. F. R. (1991). Effects of cycloheximide on B-chronic lymphocytic leukaemic and normal lymphocytes *in vitro*: induction of apoptosis. Br. J. Cancer *64*, 518–522.

Coyle, J. T., and Puttfarcken, P. (1993). Oxidative stress, glutamate, and neurodegenerative disorders. Science *262*, 689–695.

Csernansky, C. A., Canzoniero, L. M. T., Sensi, S. L., Yu, S. P., and Choi, D. W. (1994). Delayed application of aurintricarboxylic acid reduces glutamate-induced cortical neuronal injury. J. Neurosci. Res. *38*, 101–108.

Deckwerth, T. L., and Johnson, E. M., Jr. (1993). Neurotrophic factor deprivation-induced death. Ann. NY Acad. Sci. *679*, 121–131.

Deckwerth, T. L., and Johnson, E. M., Jr. (1994). Neurites can remain viable after destruction of the neuronal soma by programmed cell death (apoptosis). Dev. Biol. *165*, 63–72.

Dessi, F., Charriaut-Marlangue, C., Khrestchatisky, M., and Ben-Ari, Y. (1993). Glutamate-induced neuronal death is not programmed cell death in cerebellar culture. J. Neurochem. *60*, 1953–1955.

Duvall, E., Wyllie, A. H., and Morris, R. G. (1985). Macrophage recognition of cells undergoing programmed cell death (apoptosis). Immunology *56*, 351–358.

Dypbukt, J. M., Ankarcrona, M., Burkitt, M., Sjöholm, Å., Ström, K., Orrenius, S., and Nicotera, P. (1994). Different prooxidant levels stimulate growth, trigger apoptosis, or produce necrosis of insulin-secreting RINm5F cells: the role of intracellular polyamines. J. Biol. Chem. *269*, 30553–30560.

Filipski, J., Leblanc, J., Youdale, T., Sikorska, M., and Walker, P. R. (1990). Periodicity of DNA folding in higher order chromatin structures. EMBO J. *9*, 1319–1327.

Frandsen, A., and Schousboe, A. (1990). Development of excitatory amino acid induced cytotoxicity in cultured neurons. Int. J. Dev. Neurosci. *8*, 209–216.

Garthwaite, J., and Garthwaite, G. (1990). Excitatory Amino Acids and Neuronal Plasticity, Y. Ben-Ari, ed. (New York: Plenum Press), pp. 505–518.

Hahn, J. S., Aizenman, E., and Lipton. S. A. (1988). Central mammalian neurons resistant to glutamate toxicity are made sensitive by elevated extracellular calcium: toxicity blocked by the *N*-methyl-D-aspartate antagonist MK-801. Proc. Natl. Acad. Sci. USA *85*, 6556–6560.

Héron, A., Pollard, H., Dessi, F., Moreau, J., Lasbennes, F., Ben-Ari, Y., and Charriaut-Marlangue, C. (1993). Regional variability in DNA fragmentation after global ischemia evidenced by combined histological and gel electrophoresis observations in the rat brain. J. Neurochem. *61*, 1973–1976.

Ignatowicz, E., Vezzani, A. M., Rizzi, M., and D'Incalci, M. (1991). Nerve cell death induced *in vivo* by kainic acid and quinolinic acid does not involve apoptosis. NeuroReport *2*, 651–654.

Jacobson, M. D., Burne, J. F., King, M. P., Miyashita, T., Reed, J. C., and Raff, M. C. (1993). Bcl-2 blocks apoptosis in cells lacking mitochondrial DNA. Nature *361*, 365–369.

Jacobson, M. D., Burne, J. F., and Raff, M. C. (1994). Programmed cell death and bcl-2 protection in the absence of a nucleus. EMBO J. *13*, 1899–1910.

Jones, D. P. (1981). Determination of pyridine dinucleotides in cell extracts by high-performance liquid chromatography. J. Chromatogr. *225*, 446–449.

Kerr, J. F. R., Wyllie, A. H., and Currie, A. R. (1972). Apoptosis: a basic biological phenomenon with wide ranging implications in tissue kinetics. Br. J. Cancer *26*, 239–257.

Kure, S., Tominaga, T., Yoshimoto, T., Tada, K., and Narisawa, K. (1991). Glutamate triggers internucleosomal DNA cleavage in neuronal cells. Biochem. Biophys. Res. Commun. *179*, 39–45.

Lazebnik, Y. A., Kaufmann, S. H., Desnoyers, S., Poirier, G. G., and Earnshaw, W. C. (1994). Cleavage of poly(ADP-ribose) polymerase by a proteinase with properties like ICE. Nature *371*, 346–347.

Leist, M. F., Gantner, F., Bohlinger, I., Germann, P. G., Tiegs, G., and Wendel, A. (1994). Murine hepatocyte apoptosis induced *in vitro* and *in vivo* by TNF-α requires transcriptional arrest. J. Immunol. *153*, 1778–1788.

Leist, M. F., Gantner, F., Bohlinger, I., Germann, P. G., Tiegs, G., and Wendel, A. (1995). TNF-induced murine hepatic apoptosis as a pathomechanism of septic liver failure. Am. J. Pathol. *166*, 1–15.

Linnik, M. D., Zobrist, R. H., and Hatfield, M. D. (1993). Evidence supporting a role for programmed cell death in focal cerebral ischemia in rats. Stroke *24*, 2002–2009.

Lipton, S. A., and Rosenberg, P. A. (1994). Mechanisms of disease: excitatory amino acids as a final common pathway for neurologic disorders. N. Engl. J. Med. *330*, 613–622.

MacManus, J. P., Buchan, A. M., Hill, I. E., Rasquinha, I., and Preston, E. (1993). Global ischemia can cause DNA fragmentation indicative of apoptosis in rat brain. Neurosci. Lett. *164*, 89–92.

MacManus, J. P., Hill, I. E., Huang, Z. G., Rasquinha, I., Xue, D., and Buchan, A. M. (1994). DNA damage consistent with apoptosis in

transient focal ischaemic neocortex. NeuroReport *5*, 493–496.

Manev, H., Fararon, M., Guidotti, A., and Costa, E. (1989). Delayed increase of Ca^{2+} influx elicited by glutamate: role in neuronal death. Mol. Pharmacol. *36*, 106–112.

McConkey, D. J., Nicotera, P., Hartzell, P., Bellomo, G., Wyllie, A. H., and Orrenius, S. (1989). Glucocorticoids activate a suicide process in thymocytes through an elevation of cytosolic Ca^{2+} concentration. Arch. Biochem. Biophys. *269*, 365–370.

Meldrum, B., and Garthwaite, J. (1990). Excitatory amino acid neurotoxicity and neurodegenerative disease. Trends Pharmacol. Sci. *11*, 379–387.

Mosmann, T. (1983). Rapid colorimetric assay for cellular growth and survival: application to proliferation and cytotoxicity assays. J. Immunol. Meth. *65*, 55–63.

Newmeyer, D. D., Farschon, D. M., and Reed, J. C. (1994). Cell-free apoptosis in Xenopus egg extracts: inhibition by Bcl-2 and requirement for an organelle fraction enriched in mitochondria. Cell *79*, 353–364.

Nicotera, P., Thor, H., and Orrenius, S. (1989). Cytosolic-free Ca^{2+} and cell killing in hepatoma 1c1c7 cells exposed to chemical anoxia. FASEB J. *3*, 59–64.

Nicotera, P., Zhivotovsky, B., Bellomo, G., and Orrenius, S. (1994). Ion signalling in apoptosis. In Apoptosis, R. T. Schimke and E. Mihich, eds. (New York: Plenum Press), pp. 97–115.

Oberhammer, F., Wilson, J. W., Dive, C., Morris, I. D., Hickman, J. A., Wakeling, A. E., Walker, P. R., and Sikorska, M. (1993). Apoptotic death in epithelial cells: cleavage of DNA to 300 and/or 50 kb fragments prior to or in the absence of internucleosomal fragmentation. EMBO J. *12*, 3679–3684.

Oberhammer, F., Hochegger, K., Fröschl, G., Tiefenbacher, R., and Pavelka, M. (1994). Chromatin condensation during apoptosis is accompanied by degradation of lamin A+B, without enhanced activation of cdc2 kinase. J. Cell Biol. *126*, 827–837.

Piacentini, M., Autuori, F., Dini, L., Farrace, M. G., Ghibelli, L., Piredda, L., and Fesus, L. (1991). "Tissue" transglutaminase is specifically expressed in neonatal rat liver cells undergoing apoptosis upon epidermal growth factor stimulation. Cell Tissue Res. *263*, 227–234.

Ratan, R. R., Murphy, T. H., and Baraban, J. M. (1994). Macromolecular synthesis inhibitors prevent oxidative stress-induced apoptosis in embryonic cortical neurons by shunting cysteine from protein synthesis to glutathione. J. Neurosci. *14*, 4385–4392.

Reers, M., Smith, T. W., and Chen, L. B. (1991). J-aggregate formation of a carbocyanine as a quantitative fluorescent indicator of membrane potential. Biochemistry *30*, 4480–4486.

Savill, J. S., Fadok, V., Henson, P., and Haslett, C. (1993). Phagocyte recognition of cells undergoing apoptosis. Immunol. Today *14*, 131–136.

Schousboe, A., Meier, E., Drejer, J., and Hertz, L. (1989). Preparation of primary cultures of mouse (rat) cerebellar granule cells. In A Dissection and Tissue Culture Manual of the Nervous System, A. Shahar, J. de Vellis, A. Vernadakis, and B. Haber, eds. (New York: Alan R. Liss, Inc.), pp. 203–206.

Schramm, M., Eimerl, S., and Costa, E. (1990). Serum and depolarizing agents cause acute neurotoxicity in cultured cerebellar granule cells: role of glutamate receptor responsive to N-methyl-D-aspartate. Proc. Natl. Acad. Sci. USA *87*, 1193–1197.

Siesjö, B. K. (1992). Pathophysiology and treatment of focal cerebral ischemia. J. Neurosurg. *77*, 169–184.

Smiley, S. T., Reers, M., Mottola-Hartshorn, C., Lin, M., Chen, A., Smith, T. W., Steele, G. D., Jr., and Chen, L. B. (1991). Intracellular heterogeneity in mitochondrial membrane potentials revealed by a J-aggregate-forming lipophilic cation JC-1. Proc. Natl. Acad. Sci. USA *88*, 3671–3675.

Thomas, N., and Bell, P. A. (1981). Glucocorticoid-induced cell size changes and nuclear fragility in rat thymocytes. Mol. Cell. Endocrinol. *22*, 71–84.

Vaccarino, F. M., Alho, H., Santi, M. R., and Guidotti, A. (1987). Coexistence of GABA receptors and GABA-modulin in primary cultures of rat cerebellar granule cells. J. Neurosci. *7*, 65–76.

Wyllie, A. H. (1980). Glucocorticoid-induced thymocyte apoptosis is associated with endogenous endonuclease activation. Nature *284*, 555–556.

Wyllie, A. H., Kerr, J. F. R., and Currie, A. R. (1980). Cell death: the significance of apoptosis. Int. Rev. Cytol. *68*, 251–306.

Wyllie, A. H., Morris, R. G., Smith, A. L., and Dunlop, D. (1984). Chromatin cleavage in apoptosis: association with condensed chromatin morphology and dependence on macromolecular synthesis. J. Pathol. *142*, 67–77.

Zhivotovsky, B., Wade, D., Nicotera, P., and Orrenius, S. (1994a). Role of endonucleases in apoptosis. Int. Arch. Allergy Immunol. *105*, 333–338.

Zhivotovsky, B., Wade, D., Gahm, A., Orrenius, S., and Nicotera, P. (1994b). Formation of 50 kbp chromatin fragments in isolated liver nuclei is mediated by protease and endonuclease activation. FEBS Lett. *351*, 150–154.

Zubay, G. (1988). Biochemistry, 2nd edition (New York: Macmillan Publishing Co.).